Available online at www.sciencedirect.com

ScienceDirect

journal homepage: www.elsevier.com/locate/he

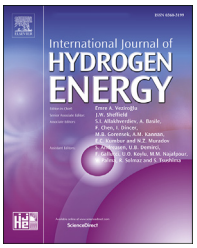

Study and characterization of the instabilities generated in expanding spherical flames of hydrogen/methane/air mixtures

M. Reyes [a,*], R. Sastre [a], F.V. Tinaut [b], J. Rodríguez-Fernández [c]

[a] Department of Energy and Fluid Mechanics Engineering, University of Valladolid, Paseo del Cauce s/n, 47011, Valladolid, Spain

[b] CMT-Motores Térmicos, Universitat Politècnica de València, 46022, Valencia, Spain

[c] Universidad de Castilla la Mancha. ETS Ingeniería Industrial (Edificio Politécnico), Avda. Camilo José Cela,3, 10371, Ciudad Real, Spain

HIGHLIGHTS

- Origin and nature of instabilities developed in spherical hydrogen/methane flames.
- Differentiate instabilities of hydrodynamic and thermal-diffusive origin.
- Instability peninsulas calculated to establish stability limits in each mixture.
- Lewis effective number determines the shape and location of instability peninsulas.

ARTICLE INFO

Article history:
Received 11 March 2022
Received in revised form
3 May 2022
Accepted 8 May 2022
Available online xxx

Keywords:
Combustion instabilities
Thermal-diffusive and hydrodynamic effect
Peninsula of instability
Cellularity
Growth rate of instabilities
Schlieren photography

ABSTRACT

In the present work an analysis of the origin and nature of intrinsic instabilities in combustion processes with different hydrogen/methane mixtures is developed. These expanding spherical flame front experiments have been developed in a cylindrical constant volume combustion bomb, which allows recording the process through Schlieren photography method.

The stability study in combustion processes has a great importance to assure their security and control, since the understanding of flame instabilities is necessary for improving the internal combustion engines performance.

To carry out this mentioned study, a review of the concepts and parameters used in spherical flame front instabilities research is first proposed, as well as a physical explanation of each concept and the relations among them.

Additionally, a methodology that aims to determine the influence of the fuel mixtures in the origin and development of the flame front instabilities is suggested. Moreover, the intrinsic effects of the combustion process, such as the thermal-diffusive and the hydrodynamic effect, are separately studied, including their individual contributions to the growth rate of instabilities which allows to determine combustion nature and to obtain the instability peninsula of each fuel mixture.

* *Corresponding author.*
E-mail address: miriam.reyes@uva.es (M. Reyes).

https://doi.org/10.1016/j.ijhydene.2022.05.063

Finally, this methodology includes a qualitative study of the cellularity phenomenon (when the instabilities develop all over the flame front), considering the parameters which influence on this phenomenon.

Introduction

Nowadays, there is an energy problem worldwide based on the one hand, on a practically exclusive dependence on fossil fuels derived from petroleum, and, on the other hand, on the effect that their use has on the environment due to the emissions generated in their combustion process. It is estimated that the transport sector is responsible for almost 30% of total CO_2 emissions in the European Union (EU), with this gas being the main cause of the greenhouse effect. A possible solution is the replacement of these CO_2-producing fuels with others with low or no carbon content such as hydrogen (H_2) or ammonia (NH_3), being more sustainable from the environmental point of view.

Prior to the introduction of any fuel mixture in a conventional engine, its behavior must be studied by isolating it from other external factors that may affect the performance of combustion, such as the turbulence that occurs in an engine due to the movement of the pistons. Constant volume combustion bombs (CVCB) allow the analysis of mixtures in laminar regime, thus facilitating the study of their nature. The above approach is at the base of this research work, in which laminar combustion of spherical flames of mixtures of H_2/CH_4/air with different percentages of hydrogen (H_2) are characterized in a CVCB with cylindrical geometry.

A fundamental aspect in the characterization of fuel combustion is the study of its stability, which consists of the analysis of the development of the instabilities inherent to the combustion process: origin, nature (thermo-diffusive or hydrodynamic, mainly), growth, etc. These can alter the morphology of the flame and affect the burning velocity. There is a growing interest in understanding and controlling the unstable behavior of cellular flames [1] and the transition to cellularity in expanding spherical flames [2–4].

There are several ways to characterize a combustion process depending on the method and resources used, but all of them aim to determine the most significant parameters that define how a combustion is developing: thermodynamic conditions, burning velocity, instabilities, and flame morphology among others. The Schlieren technique is used in this work to record the flame front development. This technique is based on the light deflection caused by density gradients [5]. It was first employed by Toepler in 1864 [6]. The Schlieren method is widely used for the study of flames in a combustion process since it allows their recording with a great clarity [7]. Thanks to the use of this technique, it is possible to study the morphology [8,9], instabilities and cellularity of the flame front, as well as its burning velocity [4,5,8,10] and, therefore, characterize the fuel mixture considered [11,12].

Spontaneous perturbations appear in flames due to various phenomena such as acoustic vibrations or pressure waves [4]. Intrinsic combustion effects cause that the amplitude of the waves on the flame front decreases or increases depending on the dominant action of those effects. The result of each effect in the flame front is the instability, independently of their stabilizing or destabilizing character [13,14]. The phenomena that can produce instabilities in the flame front (in a laminar regime) of a premixed combustion are three: volume forces, hydrodynamic effects and thermo-diffusive effects [15].

Volume forces are relevant when a less dense fluid moves towards a denser one in the opposite direction to that of a volume force (for example, gravity). Then, there appears an instability due to volume forces (also known as Rayleigh-Taylor [16]). In a flame, this occurs when the combustion products (with lower density) advance towards the fresh mixture (higher density) upwards (contrary to gravity); the flame front is then considered as a discontinuity of densities. This instability type, compared with the other two, has the lower influence on the development of the flame.

The second instability considered is the hydrodynamic one (Darrieus-Landau, DL), which is associated with the thermal expansion or density difference between the unburnt and burnt gases in a combustion process, delimited by the flame front [13,14]. The hydrodynamic effect generates destabilizing instabilities since they tend to intensify all of the flame front perturbations significantly larger than the flame front thickness (δ_l) [15,17]. Hydrodynamic instability can also be stimulated by reduced flame thickness and high pressures [18]. In addition, turbulent propagation speed can be enhanced by the onset of the hydrodynamic instability [19,20].

The thermal-diffusive effect is the cause of the third instability type that affects the combustion process in a significant way. This instability does not have a unique stable or unstable character since it involves thermal and molecular diffusivities, that have opposite results [15,21–24]. The molecular diffusivity affects the perturbations in such a way that it increases them (destabilizing contribution); on the contrary, the thermal diffusivity tends to attenuate the flame front (stabilizing contribution). This effect can be represented quantitatively by the dimensionless Lewis number (*Le*), which is the ratio between thermal diffusivity (α) and molecular diffusivity (D).

Destabilizing thermal-diffusive instability occurs when the *Le* is smaller than a critical value (when the molecular diffusivity dominates the process), and cracks and cells develop

Please cite this article as: Reyes M et al., Study and characterization of the instabilities generated in expanding spherical flames of hydrogen/methane/air mixtures, International Journal of Hydrogen Energy, https://doi.org/10.1016/j.ijhydene.2022.05.063

from the beginning on the flame front surface; otherwise, the flame should be unwrinkled at first, although after a certain time, needed for the hydrodynamic instability to appear, wrinkles can be visible [25]. In addition to the latter, the influence of the flame stretch must be considered in spherical flames. This parameter includes strain and curvature effects due to the flame geometry and always tends to attenuate the instabilities in the combustion beginning (intrinsically stable character). It should be studied together with the nature of the mixture and, specifically, the thermo-diffusive effect [24,26] represented by the Lewis number (*Le*) or better, the effective Lewis number (Le_{eff}), see Refs. [21,24,27,28], which is a weighted average of the reactants Lewis numbers.

The critical radius and the cellular radius are studied in literature to characterize the onset of instability on flames and the cellular phenomenon, respectively [24,29–33]. The dimensionless flame radius is the Peclet number (*Pe*), which is the ratio between the instantaneous radius and the flame thickness. Many definitions of critical radius can be obtained in literature, Bradley et al. [34] defined the critical radius at the instant of the appearance of the first cracks in the flame front. Bechtold and Matalon [2] identified the critical radius, for flames with effective Lewis number bigger than a critical value, as the radius beyond which the flame is unstable due to the dominance of the hydrodynamic effect when instabilities are no longer dampened, although visually it is not appreciable. This is the definition of critical radius adopted in this work, associated with the critical Peclet number (Pe_{cr}). Another definition refers to the flame radius when the flame is visibly unstable due to the development of cellularity. This radius can be called critical cellular radius, also utilized by Bradley et al. [34]. From this radius, the cellularity increases the flame front surface, which produces an augmentation in the apparent combustion burning velocity (or better, combustion rate). In the works of Jiang et al. [35] and Tinaut et al. [5] this definition for the critical radius is applied.

The understanding of hydrogen/methane combustion and flame instabilities is necessary for improving internal combustion engines performance. Previous works have been focused on the burning velocity study of hydrogen/methane mixtures [36–42]. Other studies have focused on the engine combustion [43–45]. Various researchers have investigated the cell formation in hydrogen/air flames and in mixtures of hydrogen with other hydrocarbons flames [46–49], indicating that hydrogen addition increased hydrodynamic and thermal-diffusive instabilities. Additionally, an understanding of the formation and origin of cellular instabilities in hydrogen/methane-air flames should be considered further. Jiang et al. [50] studied the cellular structure of methane/hydrogen/air flames in a spherical combustor, for various equivalence ratios and hydrogen fractions, and studied a correlation between the cellular structure and pressure. Kim et al. [51] studied cellular instabilities on expanding spherical propagation hydrogen/aire, methane/air and propane/air flames. They characterized the size of the cell, observing bigger cells due to hydrodynamic instability than the generated by the thermal-diffusive. The critical Peclet number is also affected by the initial pressure, decreasing with the increment of pressure. Zhang et al. [52] made a flame dynamics analysis of natural gas enriched with hydrogen in premixed turbulent combustion, obtaining an increment of the wrinkled structure with the turbulence intensity and with the hydrogen ratio.

Cellular instabilities enhance the global propagation rate of laminar flames and have also been studied by many researchers [30,47,53–55]. Kwon et al. [56] studied hydrogen flames at elevated pressures to identify the effects of thermal expansion ratio, flame thickness, Lewis number, and stretch rate on the generation of hydrodynamic and diffusional-thermal instabilities in the flame front. Jiang et al. [50] investigated cell formation in hydrogen/methane premixed flames and obtained a correlation between cellular structure of the flame front and pressure. Sun et al. [30] studied the cellular instabilities of hydrogen-air premixed flames at different initial conditions, showing that, for lean hydrogen/air flames, the cellular instabilities are dominated by the thermal-diffusive instability, and for stoichiometric and rich hydrogen/air flames, the cellular structure is influenced by the hydrodynamic instability. Okafor et al. [57] have developed an experimental and theoretical investigation of cellular instabilities in lean hydrogen/methane mixtures in a constant volume combustion chamber, obtaining an increment of the cellular instability and self-acceleration with the increment of the hydrogen content and mixture pressure. Hu et al. [47] observed that the increment of hydrogen in methane/hydrogen/air mixtures promotes cellularity in lean flames. Law et al. [58] studied the outward propagation and development of surface cellular instability of spark-ignited spherical premixed flames of mixtures of hydrogen, hydrocarbon, and air, showing that propane substitution moderates cell formation due to both diffusional–thermal as well hydrodynamic instabilities. Smallbone et al. [59] carried out studies of flame instability, laminar and turbulent velocity of hydrogen/air mixtures in a fan stirred combustion bomb. Wang et al. [60,61] investigated the flame front structure of syngas premixed flames. Vu et al. [1] investigate the cell formation in hydrogen/methane/monoxide – air premixed flames. Jiang et al. [50] studied the influence of pressure in the development of a cellular structure.

In present work an analysis of the origin and nature of intrinsic instabilities in spherical expanding flames of hydrogen/methane blends is developed, because there is a lack of data in literature. These spherical flame front experiments have been performed in a cylindrical constant volume combustion bomb (CylCVCB), which allows image recording through Schlieren photography method and recording the instantaneous pressure. With the methodology presented in this research, it is possible to obtain the stability maps of different combustion mixtures, which corresponds with the images directly obtained. To carry out this research, a review of the concepts and parameters used in the study of instabilities in spherical flames is first proposed, as well as a physical explanation of each concept and the relations among them. After that, the experimental installation and methodology are explained, and finally experimental results are presented for mixtures of methane/hydrogen with different percentage of hydrogen (from 0 to 100%), for two different fuel/air equivalence ratios, and initial pressure and temperature constant in all the experiments.

Please cite this article as: Reyes M et al., Study and characterization of the instabilities generated in expanding spherical flames of hydrogen/methane/air mixtures, International Journal of Hydrogen Energy, https://doi.org/10.1016/j.ijhydene.2022.05.063

Stability analysis in spherical flames

To characterize an unstable spherical flame, it is important to differentiate between the instant at which instabilities are originated (at the first stages of the combustion or in the subsequent instants of the development of the combustion process) and whether or not the evolution of the instability leads to the development to a cellular flame front.

The growth rate of spherical flame instabilities is defined as the increase in time of the relative amplitude of the perturbation (ratio between the amplitude and the instantaneous radius of the sphere) formed on the surface of the flame [14] as the joint effect of the hydrodynamic and thermal-diffusive instabilities.

When the flame radius has reached a certain value r_0 (significantly greater than the thickness of the flame, δ_l) the amplitude A of the perturbation can be non-dimensionalised with r to give a. Once perturbed variables are expanded in a spherical harmonic series, a takes the following form (adapted from Ref. [4] for coherence with the subsequent expressions for the terms appearing in it):

$$a = a_0 R^{\left(\omega + \frac{\delta_l \Omega}{r \cdot \ln R}\right)} \tag{1}$$

where a_0 is the initial dimensionless amplitude when $r=r_0$; $R=r/r_0$ is the dimensionless flame radius; δ_l is the flame front thickness ($\delta_l = \alpha/S_l$, where α is the thermal diffusivity of the mixture and S_l the laminar velocity [10]). ω is associated with hydrodynamic instability [4,21,29,32]; it is a dimensionless parameter (usually denoted as ω_{DL} in its equivalent in flat flames), that only depends on the thermal expansion σ and the dimensionless wavenumber n. Ω is associated with thermal-diffusive instability [29]; it is also dimensionless and depends on the thermal expansion, Lewis number and Zeldovich number (β) (see below). The dimensionless wavenumber n quantifies the number of waves, with a λ wavelength, that fit in a circumference of radius r ($n = \frac{2\pi r}{\lambda}$), as illustrated in Fig. 1.

The growth rate of an instability is $^1/_a\,(da/dt)$ [4,21], hereinafter identified by the letter Σ, will adopt different forms depending on the case. The general function of $\Sigma(t)$ is taken from the research of Addabbo, Bechtold and Matalon [21,32], collected in the study of Lapalme et al. [24] and represented in equation (2).

$$\Sigma(t) = \frac{1}{a}\frac{da}{dt} = \frac{1}{r}\frac{dr}{dt}\left(\omega - \frac{\delta_l}{r}\Omega\right) = \frac{1}{r}\frac{dr}{dt}\left(\omega - \frac{\Omega}{Pe}\right) \tag{2}$$

In equation (2) it is possible to see the contributions to the instability grown rate due to the hydrodynamic (ω) and thermo-diffusive ($-\frac{\Omega}{Pe}$) effects [29]. Hydrodynamic effect is always positive (contributing to instability), but the thermo-diffusive effect can increase or reduce the first, depending on the value of Ω:

$$\Omega = Q_1 + \beta\left(\frac{Le_{eff} - 1}{\sigma - 1}\right)Q_2 + PrQ_3 \tag{3}$$

Note that Ω consists of three contributions, each accompanied by a Q_i coefficient. The physical meaning of each of them is as follows: the term Q_1 brings the influence of the thermal conductivity (stable character); the second term $\beta\left(\frac{Le_{eff}-1}{\sigma-1}\right)Q_2$ represents the effect of the molecular diffusion (stable or unstable) and the term PrQ_3 (Pr is the Prandtl number) brings the effect of the viscosity (stable) [62]. The coefficients Q_1, Q_2 and Q_3 are given in Eqs. (4)–(6).

$$Q_1 = \frac{\gamma_1}{\sigma\Delta}\left[n^4(\sigma+1) + \sigma n^3(2\omega+5) + n^2(\omega\sigma - 2\sigma^2 + \sigma - 1) + n\sigma(\sigma - 7 - 3\omega - \sigma\omega) - 2\sigma(1+\omega)\right] \tag{4}$$

$$Q_2 = \frac{\gamma_2(\sigma-1)}{2\Delta}\left\{2n^4 + n^3(2\omega\sigma + 2\omega + 10\sigma - 3) + n^2\left[2\sigma\omega^2 + (5\sigma-1)\omega + 3\sigma - 2\sigma^2 - 2\right] + n\left[\sigma\omega^2(1-4\sigma) - \left(14\sigma^2+1\right)\omega + 3 - 9\sigma - 8\sigma^2\right] - 2\sigma\left(\omega^2 + 4\omega + 3\right)\right\} \tag{5}$$

$$Q_3 = \frac{2n(n^2-1)(\sigma-1)}{\sigma\Delta}\left[(n+2)(\tilde{k}(x) - \gamma_3) - 3(\tilde{\lambda}(x) - 1)\right] \tag{6}$$

where $\Delta = 2a\omega + b - 2a$. The definitions of coefficients γ_1, γ_2 and γ_3 appear in the second column of Table 1. It can be seen that the three γ_i depend on the expansion ratio σ and a function $\tilde{k}(x)$ which represents the thermal conductivity expressed in terms of the dimensionless temperature T/T_u (i.e., the flame temperature T over the unburned gas temperature T_u) and scaled by its value in the unburned gas. In order to obtain explicit expressions of γ_i that still retain the main dependence on σ, different possibilities of the variation of $\tilde{k}(x)$ can be considered: constant (order of 1), variable as $\sqrt{T}$, and variable as T. The expressions of γ_i for the three possible dependences of $\tilde{k}(x)$ appear in the additional columns of Table 1.

In the first case ($\tilde{k}(x) = 1$), with the hypothesis of constant transport properties, thermal conductivity is a constant and the influence of viscosity on the stability of the flame is minimal [21]. It is worth mentioning the formulation made by Bradley and Harper in 1994 [4] with the assumption of constant properties. Coefficients Q_i are also detailed in Bradley [3] which describes four stages in the propagation of a laminar spherical flame, these are: (1) stable laminar propagation, (2) cracking of the flame front and cell formation, (3) propagation of the cellular flame, (4) turbulent propagation.

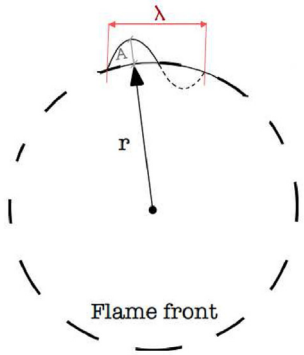

Fig. 1 – Flame radius, wave amplitude and wavelength.

Please cite this article as: Reyes M et al., Study and characterization of the instabilities generated in expanding spherical flames of hydrogen/methane/air mixtures, International Journal of Hydrogen Energy, https://doi.org/10.1016/j.ijhydene.2022.05.063

Table 1 – Analytical expressions that define the coefficients γ_i and practical as a function of the thermal conductivity [21,63].

		$\tilde{k}(x) = 1$	$\tilde{k}(x) = \sqrt{T}$	$\tilde{k}(x) = T$
γ_1	$\frac{\sigma}{\sigma-1}\int_1^\sigma \frac{\tilde{k}(x)}{x}dx$	$\frac{\sigma}{\sigma-1}\ln\sigma$	$\frac{2\sigma}{\sqrt{\sigma}+1}$	σ
γ_2	$\frac{1}{\sigma-1}\int_1^\sigma \frac{\tilde{k}(x)}{x}\ln\left(\frac{\sigma-1}{x-1}\right)dx$	$\frac{1}{\sigma-1}\int_{-\infty}^0 \ln[1+(\sigma-1)e^z]dz$	$\frac{4}{\sigma-1}\{\sqrt{\sigma}-1-\ln[0.5(\sqrt{\sigma}+1)]\}$	1
γ_3	$\frac{1}{\sigma-1}\int_1^\sigma \tilde{k}(x)dx$	1	$\frac{2(\sigma^{3/2}-1)}{3(\sigma-1)}$	$\frac{\sigma+1}{2}$

The effect of the stretch cannot be studied separately because the nature of the mixture must be considered and, specifically, the thermo-diffusive effect reflected in the ratio between the effective Lewis number Le_{eff} in a mixture, and the critical Lewis number of the combustion (Le_{eff*}). Equation (7) shows this latter parameter, where β is the Zeldovich number; as for Q_1 and Q_3, they must be evaluated for the critical radius or Peclet number according to equations (4) and (6).

$$Le_{eff*} = 1 - \frac{\sigma-1}{\beta Q_2}(Q_1 + Q_3 Pr) \tag{7}$$

As it was explained before, if in a fuel mixture $Le_{eff}<Le_{eff*}$, it means that the thermo-diffusive effect is destabilizing, and instabilities grow from the beginning. On the contrary, in combustions with $Le_{eff}>Le_{eff*}$ the thermo-diffusive effect is stabilizing and, therefore, the only effect capable of increasing instabilities is the hydrodynamic one.

It is possible to obtain the curves for the growth rate of the instability Σ when the values of Eq. (2) are represented versus the wavenumber n or alternatively the wavelength of the perturbations λ for a particular flame front radius or time [2,4,64], as can be seen in Fig. 2, where it is possible to see two regions: stable and unstable. Both zones are separated by the value of $\Sigma = 0$, the stability limit for a spherical flame. The dotted line corresponds with the critical radius r_{cr} from which there are certain wavelengths whose growth rate is positive (unstable flame).

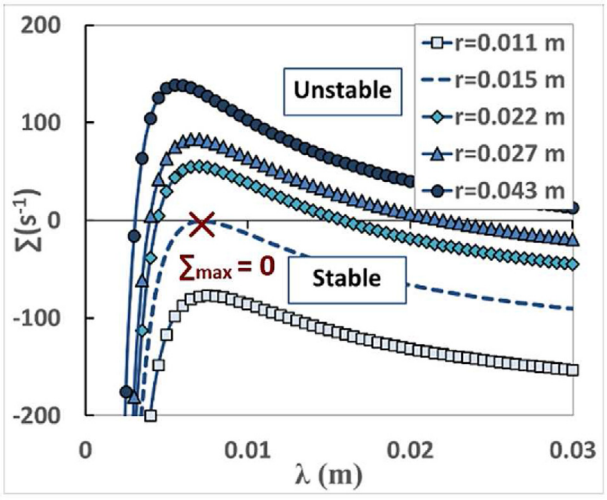

Fig. 2 – Instability growth rate curves for a given flame radius r as a function of the perturbation wavelength.

Experimental apparatus and procedure

Experimental setup

In this research work, experiments were conducted in a cylindrical constant volume combustion vessel (CylCVCB) [5], with the following dimensions: diameter 114 mm and height 135 mm, to investigate the combustion development and in particular, instabilities and the onset of cells in the flame surface, see Fig. 3. The combustion chamber was designed with two optical windows made of fused silica on the sidewalls of the cylinder. The installation is instrumented to measure instantaneous pressure during the combustion (piezoelectric pressure transducer Kistler type 7063) and to register the flame development with a high-speed Schlieren photography system: flame images were recorded using a high-speed camera Phantom V210 at 7000 frames per second (resolution 832 × 800 and exposure time of 10 ms).

Hydrogen, methane and air are individually introduced from pressure tanks using a partial pressure method, and an ignition system starts the combustion at the center of the combustion chamber (for more information about the experimental installation see Ref. [5]).

An algorithm is used to process the images obtained with the Schlieren technique (high-speed camera), to obtain the time evolution of the flame radius and to study the cellular structure which appears as a wrinkling of the flame surface. Radius evolution is obtained through frame by frame processing, after background removal, binarization and thinning transformation to highlight the borders between cells, as it is explained in detail in Ref. [5], obtaining the instantaneous position of the flame front (with a random sample consensus algorithm programmed in Matlab) and identifying the cells that appear in the flame during de combustion development.

Instantaneous pressure is registered inside the combustion chamber, and it is analyzed by means of a two-zone diagnosis model, with the aim of obtaining burning velocity, Lewis number and effective Lewis number (Le and Le_{eff}), thermal expansion σ, instability growth rate Σ, and the rest of the parameters necessary to study the instability grown rate and their coefficients, explained in detail in previous sections.

Please cite this article as: Reyes M et al., Study and characterization of the instabilities generated in expanding spherical flames of hydrogen/methane/air mixtures, International Journal of Hydrogen Energy, https://doi.org/10.1016/j.ijhydene.2022.05.063

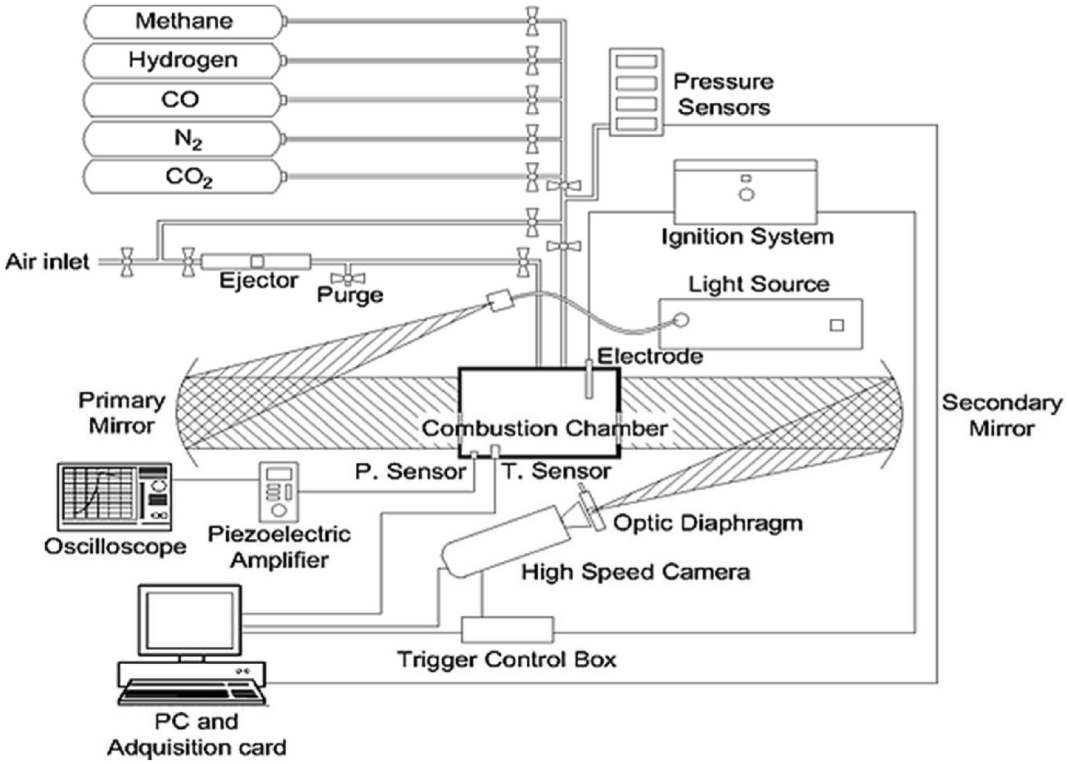

Fig. 3 – Schematics of the experimental setup.

Methodology

In this research work, mixtures of H_2/CH_4 with different percentages of hydrogen (varying from 0, 20, 50, 80 and 100%) are analyzed to determine the influence of hydrogen addition on the stability of a flame, specifically on the origin and nature of the instabilities intrinsic to a combustion process. To isolate the effect of hydrogen from other possible influencing variables, two groups of experiments with stoichiometric and lean fuel/air ratio ($\Phi = 1$ and $\Phi = 0.7$) have been selected; with an initial pressure of 0.1 MPa, and an initial temperature of 323 K. The first group ($\Phi = 1$) has been studied to identify the influence of the hydrogen in the flame stability analysis (stability limits, combustion nature, instabilities, and cellularity). The aim of the second group is to study the impact of lean equivalence ratio on the stability analysis, as well as the effect of the hydrogen content, by comparing the results with those of stoichiometric equivalence ratio.

The stability study in flames of H_2/CH_4 – air mixtures is made by examining four fundamental characteristics of a spherical flame: stability limits related to perturbations wavelength λ, flame nature, instabilities growth rate Σ and the cellularity phenomenon. In this section, it is briefly explained the meaning of each one of them and their main goals. These four characteristics are developed and applied to the selected experiments in the section corresponding to results.

- Stability limits related to perturbations wavelength (λ)

To study the stability limits related to the wavelength of the perturbations (λ) it is useful the graphical representation of the stability limits of a flame, which is called stability curve or instability peninsula [13]. Fig. 4i shows an example of this chart where the wavenumbers for which instabilities growth rate is zero ($\Sigma = 0$) are plotted versus the Peclet number. Similarly, instead of the Peclet number, the flame radius could also be utilized (this is employed in the results section of this paper).

These values conform a region that contains the wavenumbers of all the perturbations that experience an increment of their amplitude at a certain flame Peclet number (or radius) since their growth rate is positive ($\Sigma > 0$); therefore, it is called the unstable region (the blue one). The other area is the stable region, in which the growth rate of the perturbations is negative ($\Sigma < 0$) and consequently the waves are attenuated. It should be noted that the nose of the peninsula corresponds to the critical Peclet number (or critical flame radius) from which the flame enters in the unstable region. For a Peclet number larger than the critical value, there is a series of growing perturbations defined by their wavenumbers (wavelengths) between n_{max} (or λ_{min}) and n_{min} (or λ_{max}), while all those which are outside this range are decreasing. Fig. 4ii shows a growth rate curve for a given Peclet number in which these limits are marked. These maximum and minimum values fulfill the following condition for each Peclet number (and associated flame radius):

$$\Sigma = 0 = \frac{1}{a}\frac{da}{dt} = \frac{1}{r}\frac{dr}{dt}\left(\omega - \frac{\delta_l}{r}\Omega\right) \Rightarrow \omega - \frac{\Omega}{Pe} = 0 \Rightarrow \left[Pe = \frac{\Omega}{\omega}\right] \quad (8)$$

Fig. 4iii contains a joint representation of the information of the instability growth rate curve for a given Peclet number and the instability peninsula.

Please cite this article as: Reyes M et al., Study and characterization of the instabilities generated in expanding spherical flames of hydrogen/methane/air mixtures, International Journal of Hydrogen Energy, https://doi.org/10.1016/j.ijhydene.2022.05.063

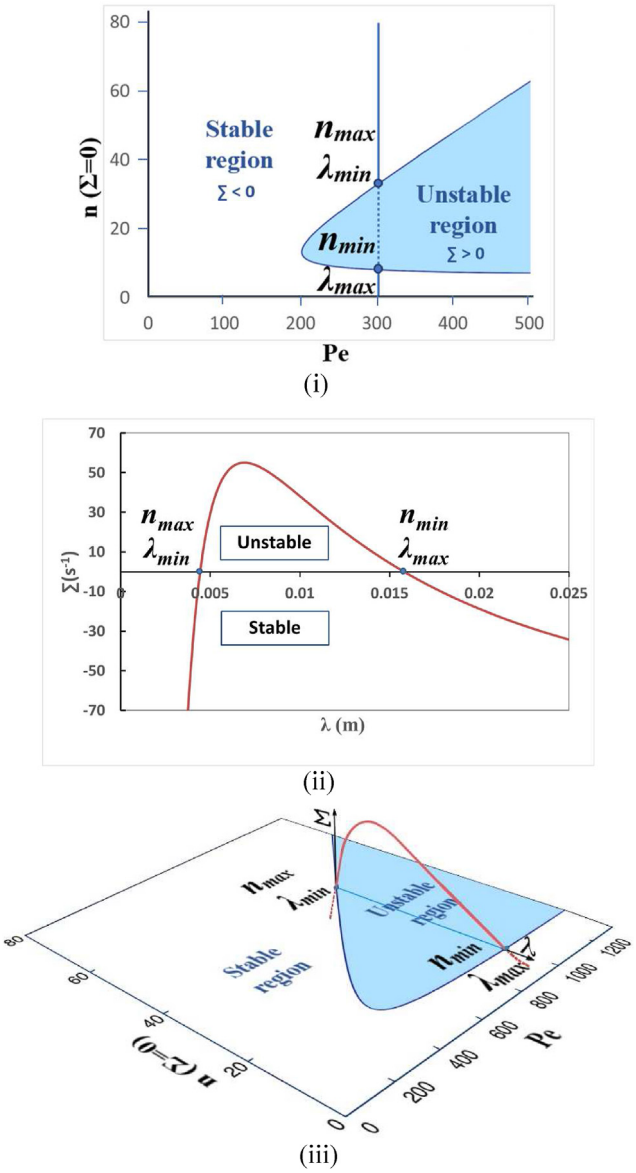

Fig. 4 – Schemes of the stability curve.

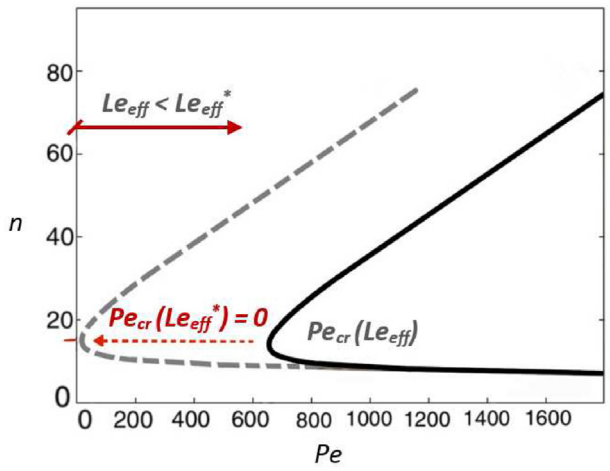

Fig. 5 – Instability peninsulas for two mixtures with different values of Le_{eff}.

- Flame stability nature.

A combustion is considered intrinsically unstable when the flame front instabilities appear and grow already from the beginning of the process, i.e., if the instability growth rate is positive ($\Sigma > 0$) at the first states of the combustion. On the contrary, if the instabilities begin to grow only after the flame radius has reached a certain value (even if it is small), a combustion is considered stable. Therefore, the combustion stability character is defined by the instabilities growth rate in the first stages of the process. As mentioned before, the hydrodynamic effect has always a destabilizing character. However, the thermal-diffusive effect could be stabilizing (counteracting the hydrodynamic effect together with the flame stretch) or destabilizing (increasing the hydrodynamic effect), meaning that the combustion stability nature is strongly dependent on this second effect.

This section aims to characterize the combustion nature and the morphology of a stability curve derived from an unstable combustion.

With the objective of identifying the stability nature of a flame, the value of its effective Lewis number must be compared with the value of its critical effective Lewis number. If the effective Lewis number value is greater than the critical one ($Le_{eff} > Le_{eff^*}$) the combustion is stable at the beginning, its instability peninsula is located to the right of the vertical axis, the instabilities have a hydrodynamic source and start to grow only once the Peclet number has a value higher than 0. Otherwise, when $Le_{eff} < Le_{eff^*}$, the combustion has an unstable nature, the instabilities arise from the thermal-diffusive effect already from the beginning (in addition to the hydrodynamic contribution.

Following the previous approach, the limit between the stable and unstable combustion is well marked by the effective Lewis number whose critical value is, in general, close to 1. In Fig. 5 two instability peninsulas for different Lewis effective numbers are presented. When the Lewis number is equal to its critical value ($Le_{eff} = Le_{eff^*}$), the peninsula *nose* touches the vertical axis, i.e., the critical Peclet number of the combustion is equal to zero (broken line in Fig. 5). When the Lewis number is lower than its critical value ($Le_{eff} > Le_{eff^*}$), the peninsula is displaced to the right in the figure.

- Instabilities growth rate and relative contributions of hydrodynamic and thermal-diffusive effects.

As previously mentioned, the influences of hydrodynamic and thermal-diffusive contributions are reflected on the instabilities growth rate (see Eq. (2) and Eq. (3)). The thermal-diffusive effect has more influence at the primary stages of the combustion process, since it is inversely proportional to the Peclet number ($-\frac{\sigma}{Pe}$). When the flame radius increases, this effect loses importance, and the growth rate is dominated by the hydrodynamic effect (ω). Consequently, the more stabilizing power the thermal-diffusive contribution has, the later the instabilities due to the hydrodynamic contribution appear. According to the above, regardless of the combustion

Please cite this article as: Reyes M et al., Study and characterization of the instabilities generated in expanding spherical flames of hydrogen/methane/air mixtures, International Journal of Hydrogen Energy, https://doi.org/10.1016/j.ijhydene.2022.05.063

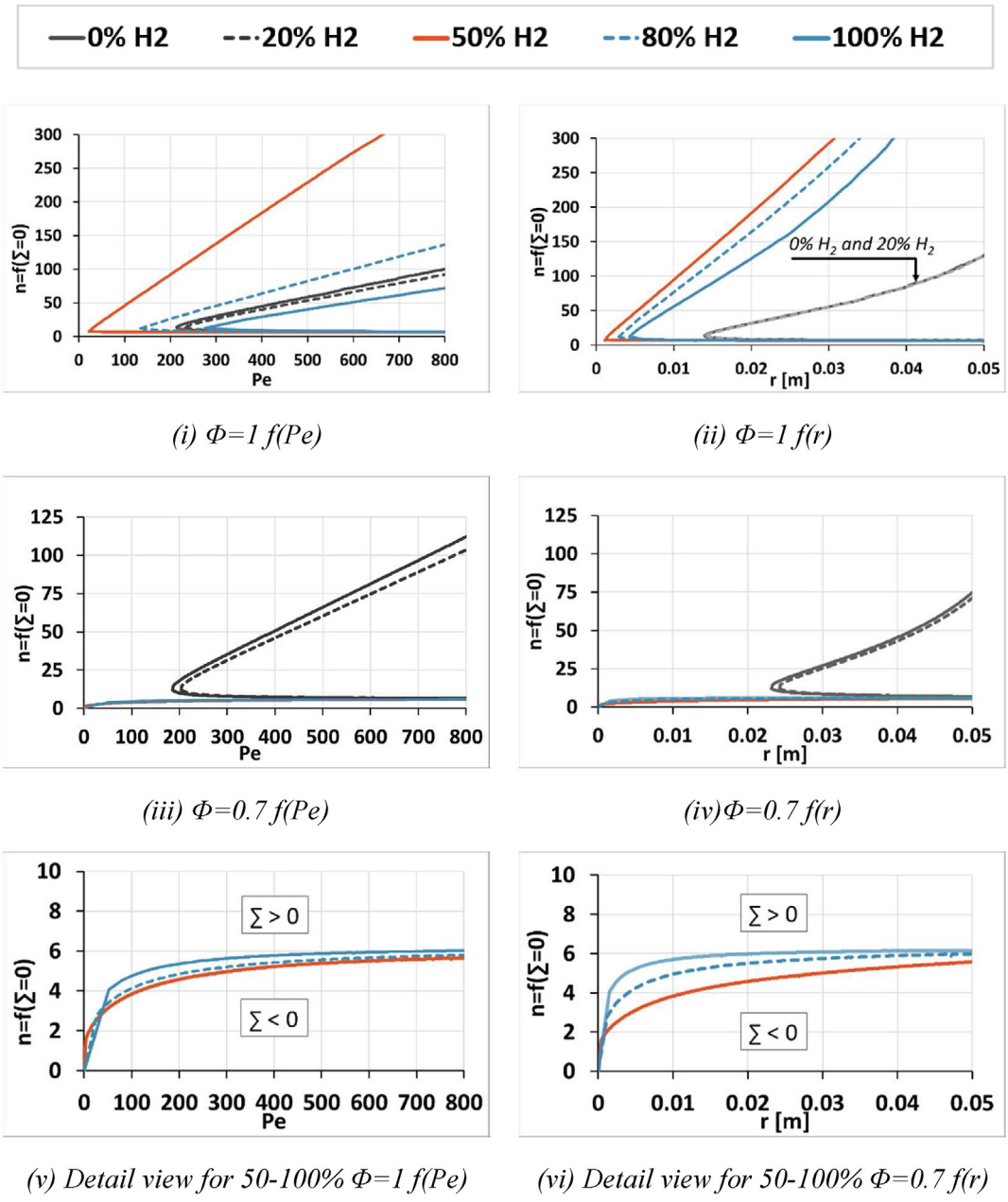

Fig. 6 – Instability peninsulas.

nature, all the flames would visibly develop instabilities in a combustion chamber with an infinite size.

- Cellularity development.

The cellularity phenomenon is the visible consequence of the full development of the instabilities in a flame front. At a certain radius, the waves amplitudes are so big that they instantly break down the flame front structure in such a way that cells are spread all over the flame surface in a perceptible way, which can be recorded by the photographic schlieren technique. A qualitative analysis of the flames can be carried out through the study of those images in order to establish the more- and less-determinant parameters on the apparition and development of the cellularity phenomenon.

Results of the stability of hydrogen/methane flames

In this section results of the stability of hydrogen-methane flames are presented for different percentages of hydrogen in the flame mixture and for two different fuel/air equivalence ratios: stoichiometric and lean mixture ($\Phi = 0.7$).

For all cases, the values of the expansion ratio σ are calculated for each time. The values of each mixture effective

Please cite this article as: Reyes M et al., Study and characterization of the instabilities generated in expanding spherical flames of hydrogen/methane/air mixtures, International Journal of Hydrogen Energy, https://doi.org/10.1016/j.ijhydene.2022.05.063

Lewis number are the corresponding to the critical radius for the stable ones and to the initial radius for those unstable, always in the unburned side. The critical Lewis number is calculated according to Eq. (7).

Stability limits

In Fig. 6 the stability maps versus the Peclet number (left) and the flame radius (right) are presented for all the experiments developed. Comparing these two representations, it can be removed the flame thickness influence. In Fig. 6i and 6ii stability curves are presented for the experiments developed at stoichiometric fuel/air equivalence ratio for different hydrogen content (0%, 20%, 50%, 80% and 100%). It can be seen that both peninsulas of the mixtures with 50% H_2 for Φ=1 are at the left of the chart with the lowest value of the critical Peclet number or flame radius (corresponding to their noses). According to the above mentioned, this means that the instabilities grow almost from the combustion beginning but this does not correspond necessarily with an earlier apparition of a cellular flame, as explained later.

The peninsulas obtained for the rest of fuel compositions are different depending on if they are plotted versus the Peclet number or flame radius. It can be seen in Fig. 6i and 6ii that the percentage of hydrogen affects significantly to the stability limits but not in a proportional way. Comparing the maps plotted versus the Peclet number and versus the flame radius (Fig. 6i and 6ii) it is possible to see the influence of the flame front thickness, especially for the combustions with 80% and 100% of hydrogen, since they have bigger Peclet numbers for the same radii (thinner flame front thickness). In Fig. 6ii it can be observed that the development of instabilities occurs at smaller radii for the medium and high hydrogen content mixtures (50, 80 and 100% of H_2) than for those with high methane content (20 and 0% of H_2). Contrasting Fig. 6i and 6ii shows that the flame thickness decreases with increasing hydrogen content: for the same Peclet number a smaller radius is obtained.

Instability peninsulas versus Peclet number for combustions under lean-fuel conditions are presented in Fig. 6iii, 6v. First thing to notice is that the experiments with low hydrogen content are slightly displaced to the left compared to those with stoichiometric-fuel conditions (i.e., slightly smaller values of the critic Peclet number). As for the medium and higher hydrogen content mixtures, their peninsulas are completely different since now they are unstable combustions from their origin. The morphology of this curves is just a line, meaning that the growth rate curves ($\Sigma = f(n)$) only have one root, i.e., only one value of the wavenumber (n) fulfils $\Sigma = 0$ (instead of the two that the stable combustions have with a peninsula shape); the unstable region corresponds, consequently, with the upper part of the graph shown in Fig. 6v and the stable region is the inferior part.

When the instability peninsulas are represented versus the flame radius (Fig. 6iv and 6vi) the peninsulas for the lower hydrogen content mixtures are displaced to the right, i.e., their critical radius are bigger compared to those of the stoichiometric case. This suggest that mixtures with 0 and 20% of H_2 (i.e., methane is dominant) are more stable at lean conditions than at stoichiometric conditions. For high and medium hydrogen contents (dominant hydrogen) the tendency is the same, independently of if the instability curves are represented versus the Peclet number or flame radius (see Fig. 6v and 6vi).

Flame stability nature

The comparison of the effective Lewis number, Le_{eff}, (calculated with mixture properties) with the critical value Le_{eff^*} (calculated by means of Eq. (7)) provides the key to know if a mixture is intrinsically stable or not. For this reason, the values of these two parameters, in each combustion process, are plotted together in Fig. 7. All the stoichiometric mixtures studied in this research work are stable in their origin, since all the Lewis numbers represented in Fig. 7 (i) are bigger than its critical value ($Le_{eff}>Le_{eff^*}$). Comparing this Figure with the instability peninsulas (Fig. 6) it can be said that the closer the two Lewis number are, the more to the left the peninsula is and the less stabilizing capability the thermal-diffusive effect has.

The evolution of the Lewis number and its critical value based on the hydrogen content can be related to the dominant fuel in each case. Traditionally, for mixtures of methane/hydrogen/air, has been accepted that hydrogen is dominant when its content is 50% and higher, while in case of a lower hydrogen content methane is dominant. This can be seen in the research of burning velocities of this types of mixtures carried out by Reyes et al. [36].

These results are compatible with the experimental behavior observed for stoichiometric mixtures in this study. It can be seen in the stability maps (Fig. 6), especially in those represented versus the flame radius (Fig. 6ii and 6iv) or in the Lewis numbers (Fig. 7i), that the shape of

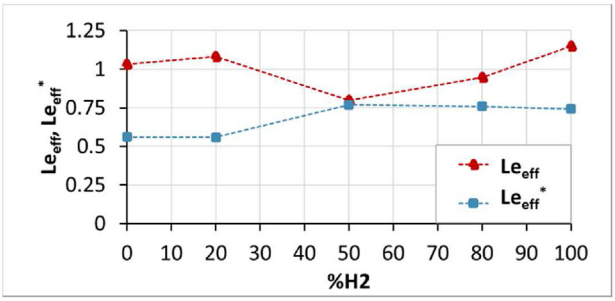

(i) Φ=1

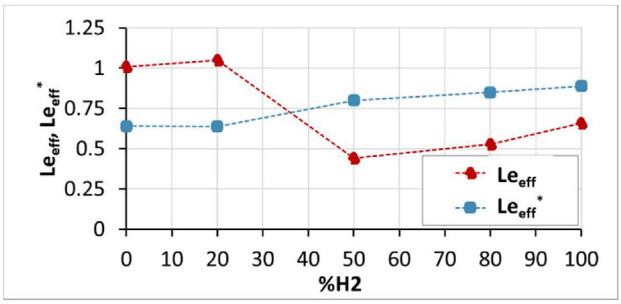

(ii)Φ=0.7

Fig. 7 – Le_{eff} and Le_{eff^*} versus the percentage of hydrogen in the fuel mixture.

Please cite this article as: Reyes M et al., Study and characterization of the instabilities generated in expanding spherical flames of hydrogen/methane/air mixtures, International Journal of Hydrogen Energy, https://doi.org/10.1016/j.ijhydene.2022.05.063

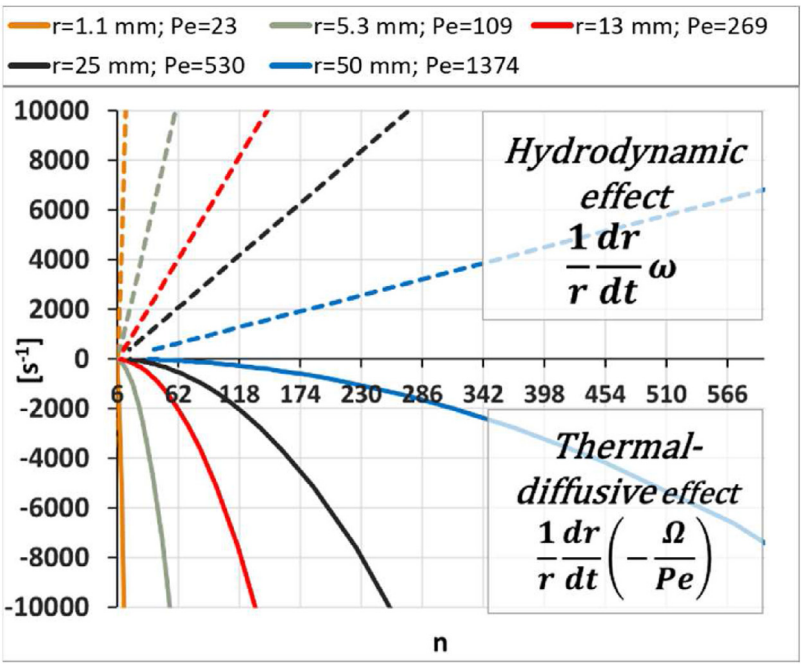

(i) Contributions to the instability growth rate Σ for Φ=1

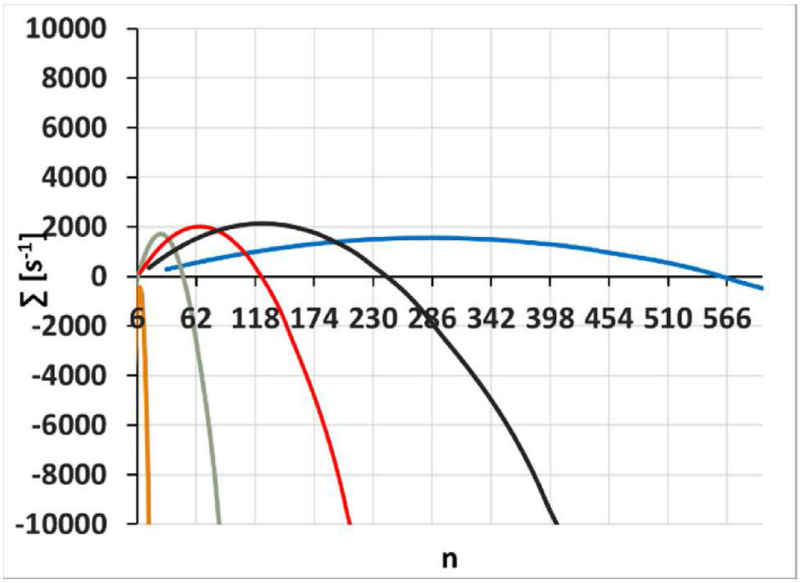

(ii) Net value of instability growth rate Σ for Φ=1

Fig. 8 – Components of instability growth rate Σ in a stoichiometric mixture with 50%H_2/CH_4.

the peninsulas for the experiments with 0 and 20% of hydrogen (i.e., dominant methane) are very similar, as well as their Lewis numbers. Nevertheless, there is a great change in the experiments with the 50% of hydrogen (i.e., hydrogen is dominant). In the study made by Hu et al., in 2009 [65], they explain this situation by considering the relative equivalence ratio according to the content of each component in the fuel mixture. By comparing Fig. 6i and 6ii and Fig. 7i, it can be seen that all stoichiometric mixtures are intrinsically stable. This means that the flame radius must appreciably grow before the instabilities appear on the flame surface.

Please cite this article as: Reyes M et al., Study and characterization of the instabilities generated in expanding spherical flames of hydrogen/methane/air mixtures, International Journal of Hydrogen Energy, https://doi.org/10.1016/j.ijhydene.2022.05.063

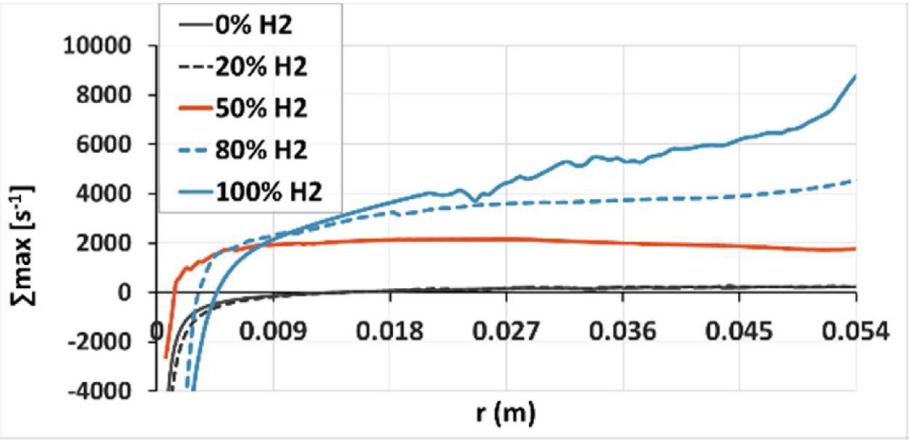

Fig. 9 – Maximum values of the instability growth rate Σ_{max} in a stoichiometric mixture with 50%H_2/CH_4.

However, in the study of the experiments under lean-fuel conditions, two of the mixtures are intrinsically stable (the ones with 0% and 20% of H_2 in which methane is dominant) and three of the mixtures are intrinsically unstable (the ones with 50, 80 and 100% of H_2 in which hydrogen is dominant). This stability change can be observed in Fig. 6iii-6vi and is also reflected in Fig. 7ii, where only two of the mixtures have a Lewis number greater than their critical value. Among the other three experiments, the combustion with 50% H_2 has the lowest value of the Lewis effective number, which corresponds with the lowest curve in Fig. 6vi and the lowest point in Fig. 7ii.

Instability growth rate (Σ) and contributions of hydrodynamic and thermal-diffusive effects for the 50%H_2/CH_4 mixtures

In Fig. 8i the independent contributions of hydrodynamic and thermal-diffusive effects on the instabilities growth rate (Σ, *Eq.*2) are represented as a function of the wavenumber n for the stoichiometric combustion of a 50%H_2/CH_4 mixture. The two contributions of the instability growth rate are calculated from the wavenumber $n = 6$, for which the wavelength is of the order of the flame radius, see Fig. 1. Even though this mixture is close to its stability limit, the thermal-diffusive contribution still has a stabilizing effect (it is always negative). As the flame radius increases, the stabilizing power of thermal-diffusive effect becomes weaker and drops its capability to neutralize the hydrodynamic instabilities, resulting in the apparition of cells on the flame front.

The sum of these two effects is the net growth rate Σ, which is displayed in Fig. 8 ii. It is worth recalling that the critical radius (or critical Peclet number) of a combustion is characterized for a maximum value of the instabilities growth rate equal to 0. According to the mentioned above, for this experiment the critical radius is between 1.1 mm and 5.3 mm (Peclet number between 23 and 109). For the flame radius equal to 1.1 mm, the values of the curve $\Sigma(n)$ are negative for all wavenumbers, while for the radius equal to 5.3 mm, there is a range of wavenumbers with positive values. This means that the flame with $r = 1.1$ mm and $Pe = 23$ is intrinsically stable, while when the flame radius grows ($r = 5.3$ mm and $Pe = 109$, and above) there is a range of wavenumbers, with the associated maximum and minimum wavelengths, for which instabilities can develop [66].

Fig. 9 represents the maximum values of the growth rate Σ for each radius in all the stoichiometric mixtures. This figure shows that the experiment with 50% of H_2 has the fastest initial instabilities growth, as its thermal-diffusive effect has a weaker stabilizing power. Once the radius increases and is bigger than 9 mm, the experiments with a higher hydrogen content (dotted and continuous blue lines) are those that also have higher values of the instabilities growth rate. The two mixtures with lower hydrogen content (0 and 20% H_2) also have lower growth rates, confirming that the hydrogen content is an influencing parameter for the instabilities development. In this figure it is again clear that there are two behaviors depending on the dominant fuel: the experiments with lower hydrogen content (0 and 20% of H_2) with dominant methane; and the experiments with dominant hydrogen (50, 80 and 100% of H_2).

In Fig. 10i and ii the instability growth rate and the separate contributions of hydrodynamic and thermal-diffusive effects for the lean mixture of 50%H_2/CH_4 are represented in order to compare with the previous results for stoichiometric mixtures).

On the one hand, the hydrodynamic effect follows a similar pattern in both cases (Fig. 8ii and 10ii), but, for the equivalence ratio of 0.7, the values are lower for the same radius and wavenumber because both thermal expansion σ and flame speed ($S_n = dr/dt$) are lower than in the stoichiometric case. On the other hand, the thermal-diffusive effect has an opposite trend (see Figs. 8i and 10i), since in the lean case it is destabilizing (positive increasing values), while in the stoichiometric case it is stabilizing (negative values).

As a result of the behavior of the two contributions studied, the net growth rate Σ curves of an unstable combustion are always increasing (see Fig. 10iii). That means that is not possible to study and compare their maximum values for each radius as it was done for the stoichiometric case.

Please cite this article as: Reyes M et al., Study and characterization of the instabilities generated in expanding spherical flames of hydrogen/methane/air mixtures, International Journal of Hydrogen Energy, https://doi.org/10.1016/j.ijhydene.2022.05.063

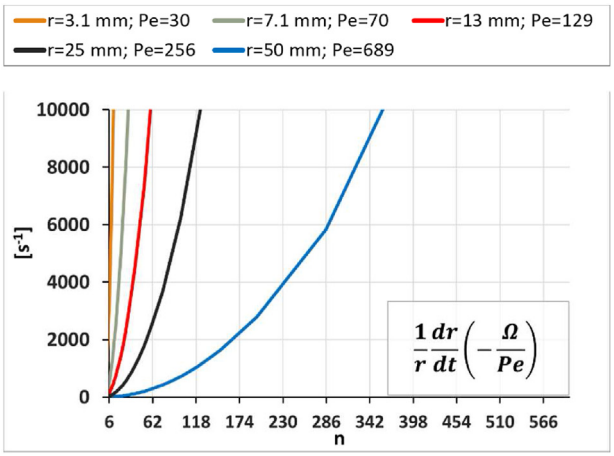

(i) Contribution of thermal-diffusive effect.

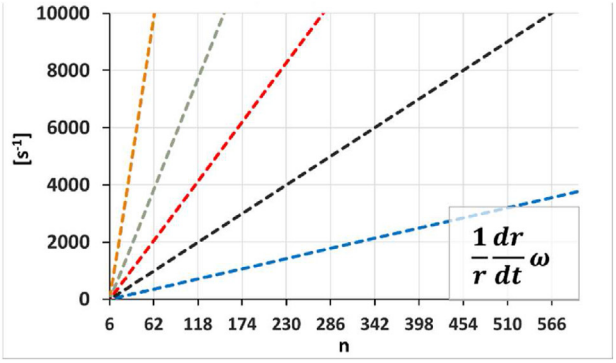

(ii) Contribution of hydrodynamic effect

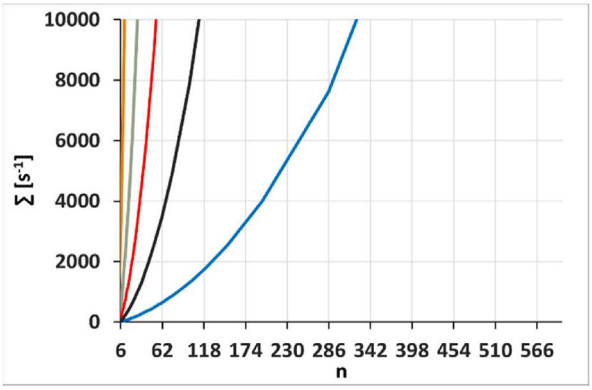

(iii) Net instability growth rate Σ.

Fig. 10 – *Components of instability growth rate Σ in a lean mixture (Φ=0.7) with 50%H_2/CH_4.*

Morphological study of H_2/CH_4 flames and cellularity development

In this section the morphological study of the H_2/CH_4 flames and the apparition of cellularity are presented. Initially, the stoichiometric mixtures which develop a cellular flame front (experiments with 100%, 80% and 50% of hydrogen) are presented in Fig. 11i and 11ii and 10iii. Moreover, the low-hydrogen content flames (20% and 0% of H_2) do not become cellular in the limits set by the combustion chamber size, as it is shown in Fig. 11iv and 11v.

It is important to establish in which of the cellular flames (experiments with 50%, 80% and 100% of H_2) develops an earlier growth of this phenomenon. For this purpose, images of the flame front of these three blends with different radii are compared in Fig. 12. For the mixtures with 80% and 100% of H_2, cellularity is already formed at $r = 5$ cm, suggesting that the cellularity origin must be for a radius smaller than 5 cm. However, for the 50% H_2/CH_4 mixture while, in spite of a few cracks on the surface, a laminar flame front is still appreciated for a radius 5 cm. It should be recalled that the stability maps show that this mixture is the one in which the instabilities first start to grow (its peninsula is the most shifted to the left). However, Fig. 9 (Σ_{max}) shows that, once the flame radius has grown, experiments with higher hydrogen content have a greater growth rate than the mixture with 50% of H_2, so it is concluded that the most influencing parameter for the apparition of cellularity is the maximum growth rate rather than the critical Peclet number or critical radius (peninsula nose). In other words, the instabilities growth rate is more important for the development of a cellular flame front than the instant when they start to grow.

In Fig. 13 the images of the flame morphology for the combustions for lean mixtures are presented. It can be seen that there are also three cellular flames (the unstable ones, which correspond to the experiments with hydrogen content varying from 50% to 100%) and two laminar flames (the stable ones, experiments with 0% and 20% of hydrogen). It should be noted that the flame front with 20% of hydrogen has several cracks on its flame surface, but they do not lead to a quick appearance of cellularity.

It is important to emphasize that the cell structure of the cellular flames under lean conditions are different from those under stoichiometric conditions, due to the different origin of the instabilities. For a stoichiometric fuel/air equivalence ratio, the cellular flames have a defined spherical shape, since there are not great wrinkles in the surface and the cells (arisen from hydrodynamic instabilities) are homogeneously spread out. However, for a lean mixture (equivalence ratio 0.7), there are large-scale wrinkles (due to thermal-diffusive instabilities) combined with smaller-scale cells, that give a clustered structure aspect to the flame, see Fig. 13i,ii,iii, and 14 [66,67].

Huang S. et al. [66] explained that, in lean-hydrogen mixtures, the development of the cracks could cause early generated cells, with long wavelength. The formation of these cracks is due to external sources such the interference with the electrodes. These large-size cells keep splitting until a saturation stage, when the cells spread all over the surface. In this phase, cells cracks formed in early instants coexist with those cells instantly formed when the cellularity develops; consequently, the newest cells arrange in the early formed ones, deriving in the clustered morphology.

Comparing Figs. 12 and 14, it is possible to observe that experiments with higher hydrogen content in lean mixtures develop a flame front cellular structure at a smaller radius than the stoichiometric mixtures, which stems from the thermal diffusive origin of the instabilities.

Please cite this article as: Reyes M et al., Study and characterization of the instabilities generated in expanding spherical flames of hydrogen/methane/air mixtures, International Journal of Hydrogen Energy, https://doi.org/10.1016/j.ijhydene.2022.05.063

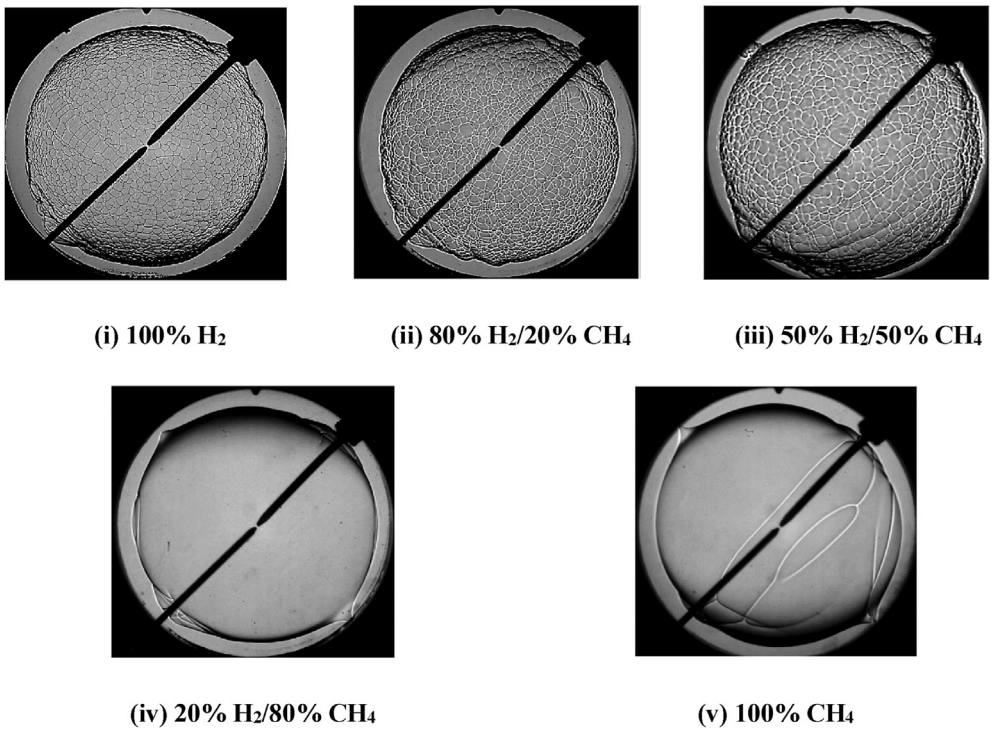

Fig. 11 – Flame morphology and cellularity apparition in some stoichiometric flames depending on H_2/CH_4 content (flame radius approx. 5 cm).

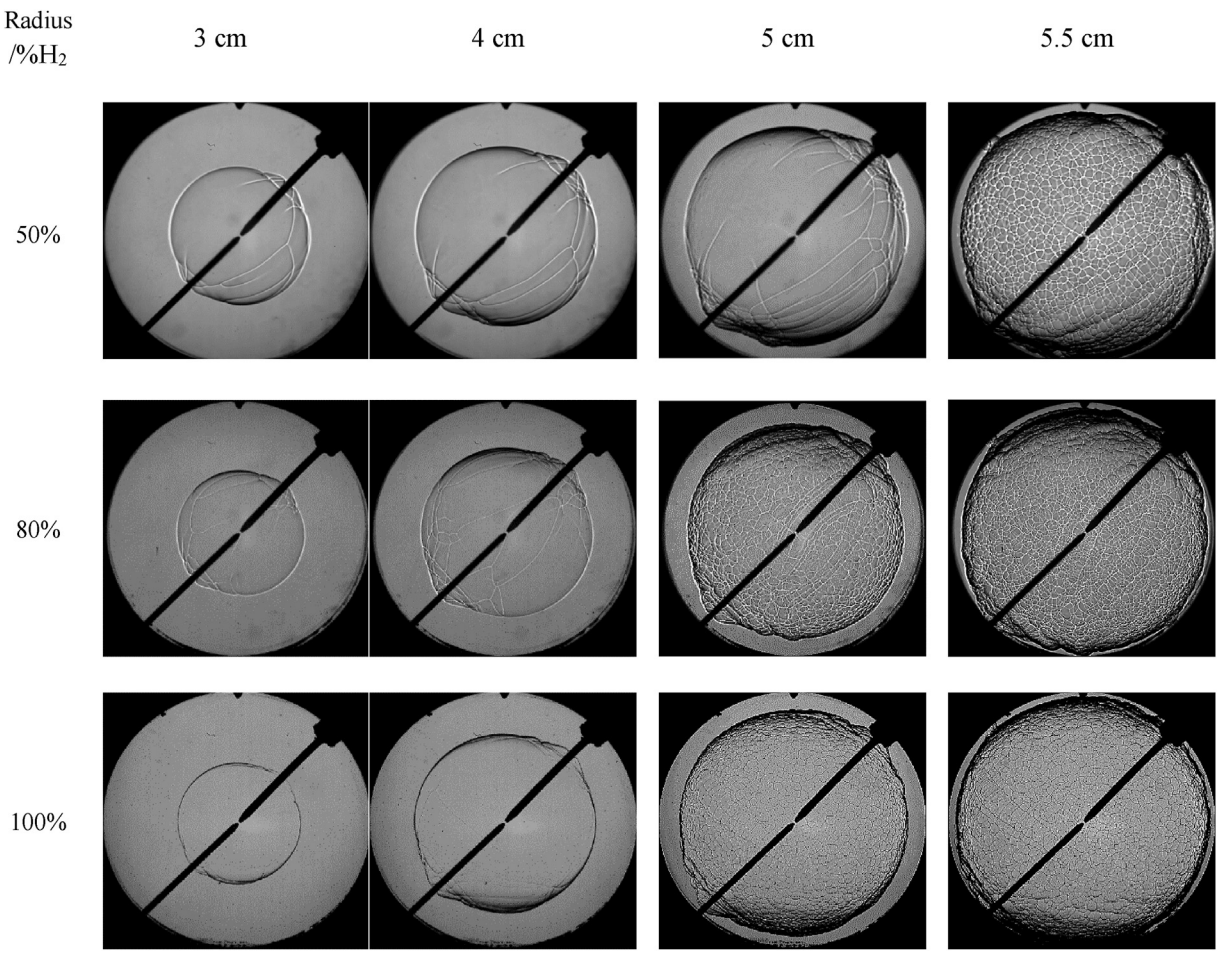

Fig. 12 – Flame morphology and cellularity apparition for the stoichiometric combustions.

Please cite this article as: Reyes M et al., Study and characterization of the instabilities generated in expanding spherical flames of hydrogen/methane/air mixtures, International Journal of Hydrogen Energy, https://doi.org/10.1016/j.ijhydene.2022.05.063

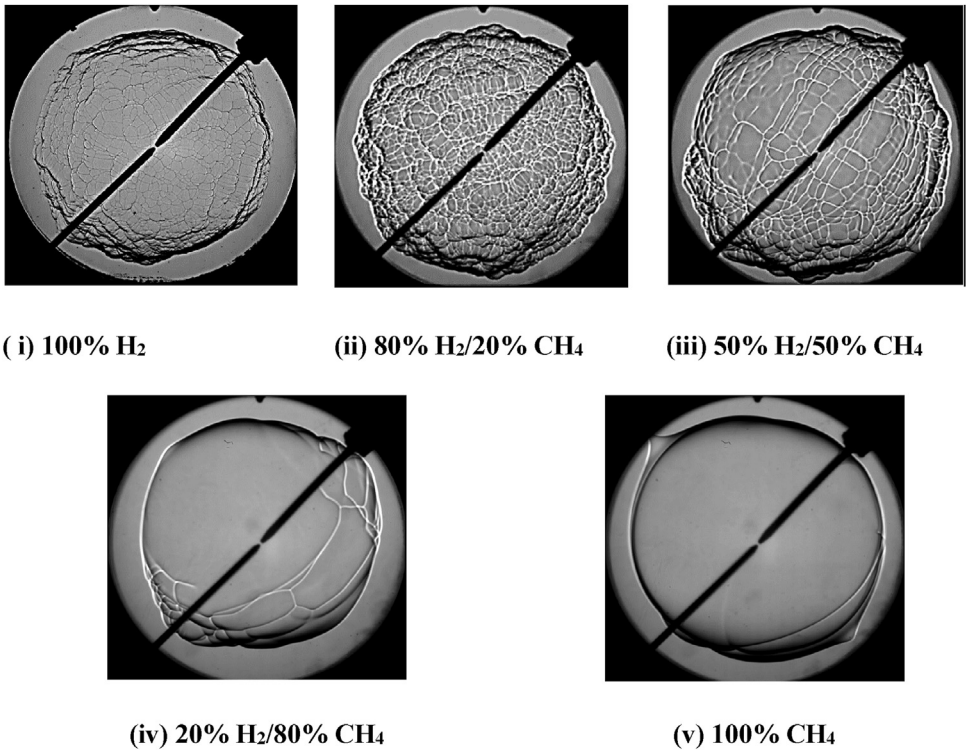

Fig. 13 – Flame morphology and cellularity apparition in some lean flames ($\Phi = 0.7$) depending on H_2/CH_4 content (flame radius approx. 5 cm).

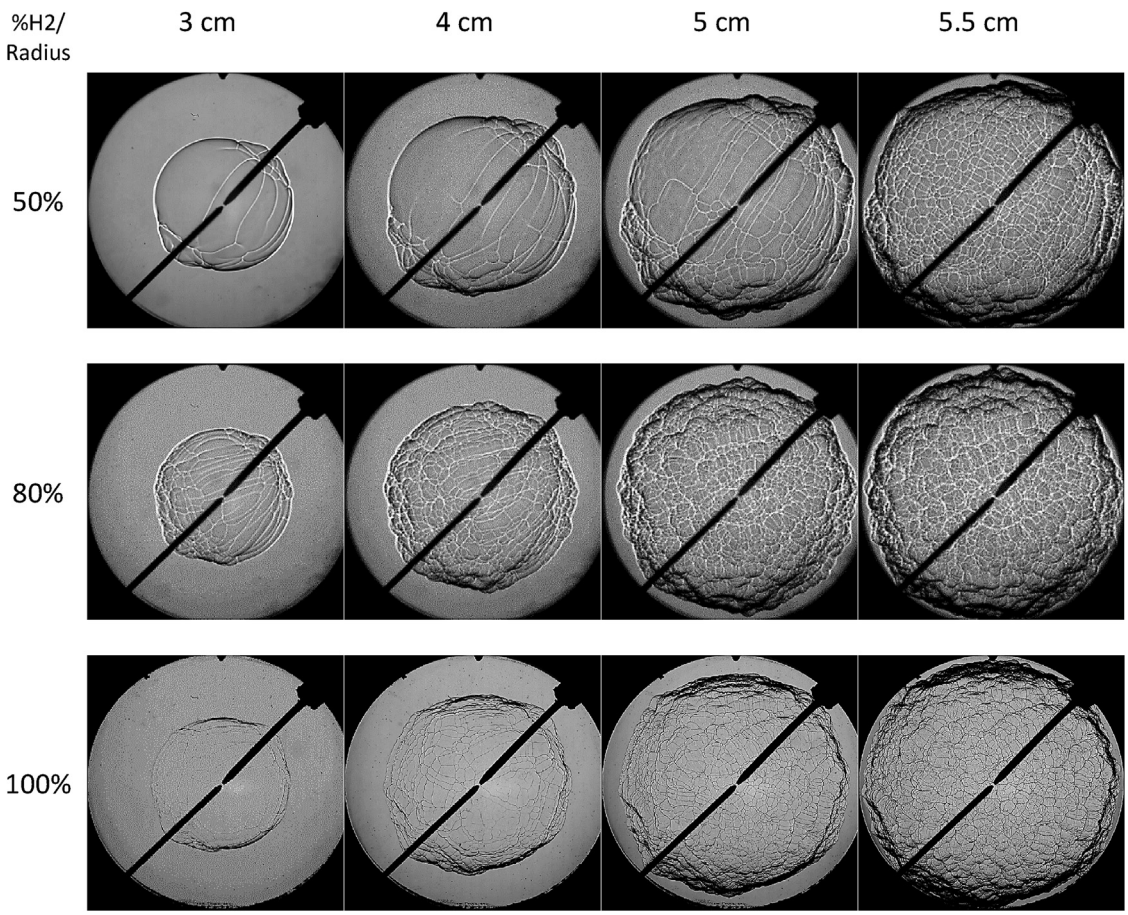

Fig. 14 – Flame morphology and cellularity apparition for the lean mixtures (Φ=0.7).

Please cite this article as: Reyes M et al., Study and characterization of the instabilities generated in expanding spherical flames of hydrogen/methane/air mixtures, International Journal of Hydrogen Energy, https://doi.org/10.1016/j.ijhydene.2022.05.063

Conclusions

In this work a study about the origin and nature of the instabilities developed in spherical flames of hydrogen/methane mixtures obtained in a cylindrical constant volume combustion bomb has been carried out. Stoichiometric and lean mixtures (with fuel/air equivalence ratio 0.7) with different hydrogen content (varying from 0 to 100%) have been analyzed in order to establish the effect of the hydrogen proportion and the fuel/air equivalence ratio on the instabilities' nature and development.

The flame nature, stable or unstable, has been studied by characterizing the instabilities developed in the flame by differentiating those associated with the hydrodynamic and the thermal-diffusive phenomena.

Stability curves or instability peninsulas have been employed to represent the wave number versus the Peclet number (and flame radius) to establish the stability limits for each mixture. Hydrogen content determines the instability peninsula shape and has a direct influence on Le_{eff}, which is a crucial parameter to determine the flame nature. The difference between Le_{eff} and Le_{eff*} affects the peninsula location in the maps of stability: for mixtures with $Le_{eff}>Le_{eff*}$, the more similar these parameters are, the more to the left the peninsula is.

When the $Le_{eff}>Le_{eff*}$ there are two stability limits, superior and inferior, and the nature of the combustion is intrinsically stable, and the instabilities developed have a hydrodynamic origin. In the opposite case, when $Le_{eff}<Le_{eff*}$, the combustion is intrinsically unstable and the origin of the instabilities is thermal-diffusive, in addition to the hydrodynamic contribution.

Instability curves for lean mixtures with higher hydrogen content show a different morphology, with only a line to separate the stable from the unstable zone, because there is only one value of wavenumber for which the growth rate is zero.

Fuel/air equivalence ratio has a great effect on the stability of those combustion processes with a significant proportion of hydrogen: in the stoichiometric case all the mixtures studied have a stable nature, meanwhile in the lean case, combustions with high content in hydrogen are unstable. In these experiments, the stability curves shape and flames morphology are greatly influenced by the fuel/air equivalence ratio, changing completely the stability curve shape from stoichiometric (peninsulas) to lean conditions (lines).

Nevertheless, the fuel/air equivalence ratio has a lower influence on the stability curves and flame morphology in mixtures in which methane is dominant, because peninsula shapes do not vary significantly with the modification of equivalence ratio.

With respect to the cellularity development, results of the morphological study of H_2/CH_4 mixtures show that cellular structure and flame front morphology are different depending on the origin of the instabilities (only hydrodynamic or also thermal-diffusive), which can have a clustered appearance. The hydrogen content influences the development of a cellular flame front, for all the cellular flames correspond to medium and high hydrogen percentages experiments. For the stoichiometric flames, the cellularity apparition is marked by the maximum values of the instability growth rate (growth velocity of the amplitude waves). For mixtures in which hydrogen is dominant, the reduction of the fuel/air equivalence ratio tends to make the flame unstable. Lean mixtures develop an early apparition of the flame front cellularity due to the thermal diffusive origin of the instability, which a clustered aspect of the cell structure.

Finally, it can be said that the maximum instability growth rate is more important for cellularity development than the flame radius (and associated Peclet number) at which instabilities are triggered.

Declaration of competing interest

The authors declare that they have no known competing financial interests or personal relationships that could have appeared to influence the work reported in this paper.

Acknowledgements

The authors would like to thank the Spanish Ministry of Science and Innovation-Agencia Estatal de Investigación, for the financial support of this investigation with the research project PID2019-106957RB-C22. This work was developed in the framework of the Research Group in Engines and Renewable Energies (MyER) from the University of Valladolid, and Institute CMT from Universitat Politècnica de València.

Abbreviations and nomenclature

A	Amplitude of the perturbation
a	Non-dimensionalised amplitude of the perturbation ($a = A/r$)
A_f	Flame front area
CVCB	Constant volume combustion bomb
CylCVCB	Cylindrical constant volume combustion bomb
D	Molecular diffusivity
$\tilde{k}(x)$	Thermal conductivity
Le	Lewis number
Le_{eff}	Effective Lewis number
Le_{eff*}	Critical effective Lewis number
n	Dimensionless wavenumber ($n = \frac{2\pi r}{\lambda}$)
p	Pressure
Pe	Peclet number
Pr	Prantl number
Qi	Coefficients of Eq. (3) and Eq. 7
r	Flame front radius
$R=r/r_0$	Dimensionless flame radius
S_l	Laminar velocity
$S_n = dr/dt$	Flame speed
T	Temperature

Greek symbols

α	Thermal diffusivity
β	Zeldovich number
δ_l	Flame front thickness ($\delta_l = \alpha / S_l$)

Please cite this article as: Reyes M et al., Study and characterization of the instabilities generated in expanding spherical flames of hydrogen/methane/air mixtures, International Journal of Hydrogen Energy, https://doi.org/10.1016/j.ijhydene.2022.05.063

γ_i	Coefficients of Eqs. (4)-6)
λ	Wavelength
Φ	Fuel/air equivalence ratio: fuel/air mass ratio over the stoichiometric fuel/air mass ratio: $\Phi = \frac{m_f/m_a}{\left(m_f/m_a\right)_{stoich}}$
ρ	Density
σ	Expansion ratio
Σ	Growth rate of an instability
ω	Parameter associated with hydrodynamic instability
Ω	Parameter associated with the thermal-diffusive instability

Subscripts

0	Reference conditions
b	Burned
cr	Critical
i	Initial
ub	Unburned

REFERENCES

[1] Vu TM, Park J, Kim JS, Kwon OB, Yun JH, Keel SI. Experimental study on cellular instabilities in hydrocarbon/hydrogen/carbon monoxide–air premixed flames. Int J Hydrogen Energy 2011;36(11):6914–24.
[2] Bechtold JK, Matalon M. Hydrodynamic and diffusion effects on the stability of spherically expanding flames. Combust Flame 1987;67(1):77–90.
[3] Bradley D. Instabilities and flame speeds in large-scale premixed gaseous explosions. Philos Trans R Soc London, Ser A: Math Phys Eng Sci 1999;357(1764):3567–81.
[4] Bradley D, Harper CM. The development of instabilities in laminar explosion flames. Combust Flame 1994;99(3):562–72.
[5] Tinaut F, Reyes M, Melgar A, Giménez B. Optical characterization of hydrogen-air laminar combustion under cellularity conditions. Int J Hydrogen Energy 2019;44(25):12857–71.
[6] Gaydon AG, Wolfhard HG. Flames, their structure, radiation, and temperature. Chapman & Hall; 1979.
[7] Settles G. Schlieren and shadowgraph techniques: visualizing phenomena in transparent media. 2002.
[8] Reyes M, Tinaut FV, Giménez B, Camaño A. Combustion and flame front morphology characterization of H2–CO syngas blends in constant volume combustion bombs. Energy Fuels 2021;35(4):3497–511.
[9] Gu G, Huang J, Han W, Wang C. Propagation of hydrogen–oxygen flames in Hele-Shaw cells. Int J Hydrogen Energy 2021;46(21):12009–15.
[10] Cao Y, Dahari M, Tlili I, Raise A. Investigation on the laminar flame speed of CH4/CO2/air mixture at atmospheric and high pressures using Schlieren photography. Int J Hydrogen Energy 2020;45(55):31151–61.
[11] Li F, Lee C-f, Wang Z, Wu H, Lu G. Schlieren investigation on impacts of duct size on macroscopic spray characteristics of ducted fuel injection. Appl Therm Eng 2020;176:115440.
[12] Yu Y. Experimental study on effects of ethanol-diesel fuel blended on spray characteristics under ultra-high injection pressure up to 350 MPa. Energy 2019;186:115768.
[13] Matalon M. Intrinsic flame instabilities in premixed and nonpremixed combustion. Annu Rev Fluid Mech 2007;39:163–91.
[14] Istratov A, Librovich V. On the stability of propagation of spherical flames. J Appl Mech Tech Phys 1966;7(1):43–50.
[15] Williams FA. Combustion theory. 1985.
[16] Bychkov V, Liberman MA. Dynamics and stability of premixed flames. Phys Rep 2000;325(4–5):115–237.
[17] Matalon M. The Darrieus–Landau instability of premixed flames. Fluid Dynam Res 2018;50(5):051412.
[18] Fogla N, Creta F, Matalon M. Influence of the Darrieus-Landau instability on the propagation of planar turbulent flames. Proc Combust Inst 2013;34(1):1509–17.
[19] Troiani G, Creta F, Matalon M. Experimental investigation of Darrieus–Landau instability effects on turbulent premixed flames. Proc Combust Inst 2015;35(2):1451–9.
[20] Reyes M, Tinaut F, Giménez B, Camaño A. Combustion and flame front morphology characterization of H2–CO syngas blends in constant volume combustion bombs. Energy Fuels 2021;35(4):3497–511.
[21] Addabbo R, Bechtold J, Matalon M. Wrinkling of spherically expanding flames. Proc Combust Inst 2002;29(2):1527–35.
[22] Law C. Propagation, structure, and limit phenomena of laminar flames at elevated pressures. Combust Sci Technol 2006;178(1–3):335–60.
[23] Clavin P, Williams F. Effects of molecular diffusion and of thermal expansion on the structure and dynamics of premixed flames in turbulent flows of large scale and low intensity. J Fluid Mech 1982;116:251–82.
[24] Lapalme D, Halter F, Mounaïm-Rousselle C, Seers P. Characterization of thermodiffusive and hydrodynamic mechanisms on the cellular instability of syngas fuel blended with CH4 or CO2. Combust Flame 2018;193:481–90.
[25] Zhang N, Zhang F, Zhong S, Peng Z, Yu J, Liu H, et al. Numerical and theoretical investigation of ethanol/air flame instability. Combust Theor Model 2020;24(6):1108–29.
[26] Kim W, Sato Y, Johzaki T, Endo T. Experimental study on the onset of flame acceleration due to cellular instabilities. J Loss Prev Process Ind 2019;60:264–8.
[27] Kim WK, Mogi T, Kuwana K, Dobashi R. Self-similar propagation of expanding spherical flames in large scale gas explosions. Proc Combust Inst 2015;35(2):2051–8.
[28] Bell JB, Cheng RK, Day MS, Shepherd IG. Numerical simulation of Lewis number effects on lean premixed turbulent flames. Proc Combust Inst 2007;31(1):1309–17.
[29] Oppong F, Zhongyang L, Li X, Xu C. Inherent instabilities in ethyl acetate premixed flames. Fuel 2021;290:120000.
[30] Sun Z-Y, Liu F-S, Bao X-C, Liu X-H. Research on cellular instabilities in outwardly propagating spherical hydrogen-air flames. Int J Hydrogen Energy 2012;37(9):7889–99.
[31] Huang S, Zhang Y, Huang R, Xu S, Ma Y, Wang Z, et al. Quantitative characterization of crack and cell's morphological evolution in premixed expanding spherical flames. Energy 2019;171:161–9.
[32] Addabbo R. The structure and stability of expanding and converging near-stoichiometric flames. New Jersey Institute of Technology; 2001.
[33] Kelley AP, Jomaas G, Law CK. Critical radius for sustained propagation of spark-ignited spherical flames. Combust Flame 2009;156(5):1006–13.
[34] Bradley D, Sheppart CGW, Woolley R, Greenhalgh DA, Lockett RD. The development and structure of flame instabilities and cellularity at low Markstein numbers in explosions. Combust Flame 2000;122(1–2):195–209.
[35] Jiang Y-H, Li G-X, Li H-M, Li L, Tian L-L. Study on the influence of flame inherent instabilities on crack propagation of expanding premixed flame. Fuel 2018;233:504–12.
[36] Reyes M, Tinaut FV, Horrillo A, Lafuente A. Experimental characterization of burning velocities of premixed methane-air and hydrogen-air mixtures in a constant volume combustion bomb at moderate pressure and temperature. Appl Therm Eng 2018;130:684–97.

Please cite this article as: Reyes M et al., Study and characterization of the instabilities generated in expanding spherical flames of hydrogen/methane/air mixtures, International Journal of Hydrogen Energy, https://doi.org/10.1016/j.ijhydene.2022.05.063

[37] Reyes M, Tinaut FV, Giménez B, Pastor JV. Effect of hydrogen addition on the OH* and CH* chemiluminescence emissions of premixed combustion of methane-air mixtures. Int J Hydrogen Energy 2018;43(42):19778–91.
[38] Miao H, Ji M, Jiao Q, Huang Q, Huang Z. Laminar burning velocity and Markstein length of nitrogen diluted natural gas/hydrogen/air mixtures at normal, reduced and elevated pressures. Int J Hydrogen Energy 2009;34(7):3145–55.
[39] Miao H, Jiao Q, Huang Z, Jiang D. Measurement of laminar burning velocities and Markstein lengths of diluted hydrogen-enriched natural gas. Int J Hydrogen Energy 2009;34(1):507–18.
[40] Hu E, Huang Z, He J, Miao H. Experimental and numerical study on laminar burning velocities and flame instabilities of hydrogen–air mixtures at elevated pressures and temperatures. Int J Hydrogen Energy 2009;34(20):8741–55.
[41] Hu E, Huang Z, He J, Miao H. Experimental and numerical study on lean premixed methane–hydrogen–air flames at elevated pressures and temperatures. Int J Hydrogen Energy 2009;34(16):6951–60.
[42] Gerke U, Steurs K, Rebecchi P, Boulouchos K. Derivation of burning velocities of premixed hydrogen/air flames at engine-relevant conditions using a single-cylinder compression machine with optical access. Int J Hydrogen Energy 2010;35(6):2566–77.
[43] Reyes M, Tinaut F, Melgar A, Pérez A. Characterization of the combustion process and cycle-to-cycle variations in a spark ignition engine fuelled with natural gas/hydrogen mixtures. Int J Hydrogen Energy 2016;41(3):2064–74.
[44] Verhelst S, Wallner T. Hydrogen-fueled internal combustion engines. Prog Energy Combust Sci 2009;35(6):490–527.
[45] Wang J, Huang Z, Miao H, Wang X, Jiang D. Study of cyclic variations of direct-injection combustion fueled with natural gas–hydrogen blends using a constant volume vessel. Int J Hydrogen Energy 2008;33(24):7580–91.
[46] Tse SD, Zhu DL, Law CK. Morphology and burning rates of expanding spherical flames in H2/O2/inert mixtures up to 60 atmospheres. Proc Combust Inst 2000;28(2):1793–800.
[47] Hu E, Huang Z, He J, Zheng J, Miao H. Measurements of laminar burning velocities and onset of cellular instabilities of methane–hydrogen–air flames at elevated pressures and temperatures. Int J Hydrogen Energy 2009;34(13):5574–84.
[48] Tang C, He J, Huang Z, Jin C, Wang J, Wang X, et al. Measurements of laminar burning velocities and Markstein lengths of propane–hydrogen–air mixtures at elevated pressures and temperatures. Int J Hydrogen Energy 2008;33(23):7274–85.
[49] Law CK, Jomaas G, Bechtold JK. Cellular instabilities of expanding hydrogen/propane spherical flames at elevated pressures: theory and experiment. Proc Combust Inst 2005;30(1):159–67.
[50] Jiang Y-H, Li G-X, Li F-S, Sun Z-Y, Li H-M. Experimental investigation of correlation between cellular structure of the flame front and pressure. Fuel 2017;199:65–75.
[51] Kim W, Imamura T, Mogi T, Dobashi R. Experimental investigation on the onset of cellular instabilities and acceleration of expanding spherical flames. Int J Hydrogen Energy 2017;42(21):14821–8.
[52] Zhang M, Chang M, Wang J, Huang Z. Flame dynamics analysis of highly hydrogen-enrichment premixed turbulent combustion. Int J Hydrogen Energy 2020;45(1):1072–83.
[53] Wu F, Jomaas G, Law CK. An experimental investigation on self-acceleration of cellular spherical flames. Proc Combust Inst 2013;34(1):937–45.
[54] Sun Z-Y, Li G-X, Li H-M, Zhai Y, Zhou Z-H. Buoyant unstable behavior of initially spherical lean hydrogen-air premixed flames. Energies 2014;7(8):4938–56.
[55] Fairweather M, Ormsby M, Sheppard C, Woolley R. Turbulent burning rates of methane and methane–hydrogen mixtures. Combust Flame 2009;156(4):780–90.
[56] Kwon O, Rozenchan G, Law C. Cellular instabilities and self-acceleration of outwardly propagating spherical flames. Proc Combust Inst 2002;29(2):1775–83.
[57] Okafor EC, Nagano Y, Kitagawa T. Experimental and theoretical analysis of cellular instability in lean H2-CH4-air flames at elevated pressures. Int J Hydrogen Energy 2016;41(15):6581–92.
[58] Law CK, Kwon O. Effects of hydrocarbon substitution on atmospheric hydrogen–air flame propagation. Int J Hydrogen Energy 2004;29(8):867–79.
[59] Smallbone A, Tsuneyoshi K, Kitagawa T. Turbulent and stable/unstable laminar burning velocity measurements from outwardly propagating spherical hydrogen-air flames at elevated pressures. J Therm Sci Technol 2006;1(1):31–41.
[60] Wang J, Zhang M, Huang Z, Kudo T, Kobayashi H. Measurement of the instantaneous detailed flame front structure of syngas turbulent premixed flames at high pressure. In: 9th asia-pacific conference on combustion, ASPACC 2013; 2013.
[61] Wang J, Zhang M, Huang Z, Kudo T, Kobayashi H. Measurement of the instantaneous flame front structure of syngas turbulent premixed flames at high pressure. Combust Flame 2013;160(11):2434–41.
[62] Zhao H, Wang J, Bian Z, Cai X, Li X, Huang Z. Onset of cellular instability and self-acceleration propagation of syngas spherically expanding flames at elevated pressures. Int J Hydrogen Energy 2019;44(51):27995–8006.
[63] Bechtold JK, Matalon M. The dependence of the Markstein length on stoichiometry. Combust Flame 2001;127(1):1906–13.
[64] Clavin P. Dynamic behavior of premixed flame fronts in laminar and turbulent flows. Prog Energy Combust Sci 1985;11(1):1–59.
[65] Hu E, Huang Z, He J, Jin C, Zheng J. Experimental and numerical study on laminar burning characteristics of premixed methane–hydrogen–air flames. Int J Hydrogen Energy 2009;34(11):4876–88.
[66] Huang S, Huang R, Zhang Y, Zhou P, Wang Z, Yin Z. Relationship between cellular morphology and self-acceleration in lean hydrogen-air expanding flames. Int J Hydrogen Energy 2019;44(59):31531–43.
[67] Huang S, Huang R, Zhou P, Zhang Y, Yin Z, Wang Z. Role of cellular wavelengths in self-acceleration of lean hydrogen-air expanding flames under turbulent conditions. Int J Hydrogen Energy 2021;46(17):10494–505.

Please cite this article as: Reyes M et al., Study and characterization of the instabilities generated in expanding spherical flames of hydrogen/methane/air mixtures, International Journal of Hydrogen Energy, https://doi.org/10.1016/j.ijhydene.2022.05.063